Distributed Amplify-and-Forward Cooperation Through Message Partitioning

Li Chen, *Member, IEEE*, Rolando Carrasco, and Ian Wassell

***Abstract*—This paper proposes a message partitioning-based distributed amplify-and-forward (MPDAF) cooperative scheme. In this scheme, the message transmitted by a user is partitioned into several equal parts, each of which will be relayed by a different user. It enables the cooperative users to share the relaying burden in a distributed network. As a result, each cooperative user deploys half of its transmission for broadcasting and the other half for relaying, maintaining both the degree of its broadcasting transmission and the spectral efficiency. Since cooperation does not require decoding and encoding processes at the relays, the system complexity of the MPDAF scheme is less than that of the space–time-coded (STC) distributed cooperative scheme, but some additional effort is required to achieve signal timing synchronization. Information theoretic analysis of the proposed scheme shows that it can achieve the same diversity–multiplexing tradeoff (DMT) performance bound as the STC scheme, achieving extra diversity gain without affecting its multiplexing gain. It is superior to the existing repetition-based distributed cooperative scheme. The scheme's outage performance substantiates this claim by showing that a significant diversity gain can be achieved. The impact of the MPDAF scheme when used in a practical coded system is analyzed, and it is shown that a diversity gain on the order of the number of relays can be achieved. We present simulation results for an MPDAF scheme employing the spectrally efficient bit-interleaved coded modulation and show that a significant diversity gain can be also achieved in a practical coded system.**

***Index Terms*—Amplify-and-forward (AF), distributed cooperation, diversity–multiplexing tradeoff (DMT), outage probability.**

I. Introduction

SPATIAL diversity is a crucial technique to improve communication quality over wireless fading channels. Concepts such as multiple-input–multiple-output systems [1] and user cooperation [2]–[4] have been introduced, owing to their ability to utilize spatial diversity and, thus, improve system performance. Among them, user cooperation can be applied more widely since it does not rely on the implementation of multiple antennas. A complete cooperative process consists of two transmissions occurring in two orthogonal time slots (TSs), namely, broadcasting transmission for source S to transmit its own message to signal destination D and relaying transmission for relay R to retransmit S's message to D. It creates a virtual multiple transmit antenna array. A number of cooperative schemes exist, for example, amplify-and-forward (AF) [4], [5] and decode-and-forward (DF) [2]–[4], [6], [7].

Laneman and Wornell [8] showed that system performance can be enhanced if cooperation is performed in a distributed manner. There are two main types of distributed cooperation, namely, repetition-based cooperation [9], [10] and space–time coded (STC) cooperation [11], [12]. In repetition-based cooperation, a number of users R take turns to retransmit S's message using either the AF or the DF mode, whereas for STC cooperation, a number of users R can simultaneously retransmit S's message assisted by an STC and operating in the DF mode. They all achieve a diversity gain on the order of the number of users R. Notice that, in this paper, we assume that the repetition-based distributed cooperation scheme is operating in the AF mode, which is denoted RDAF, since operating in the DF mode would incur high system complexity. With similar complexity, one could use STC cooperation instead and achieve a better performance, further reducing the motivation of using repetition-based cooperation in the DF mode. These schemes require multiple users for signal retransmission. However, distributed cooperation does not necessarily require constant engagement of multiple users. Bletsas *et al.* [13], [14] later showed that given a number of candidate users always selecting the best user for signal retransmission will also achieve the same diversity gain as the schemes presented in [8]. This approach is known as opportunistic cooperation. However, it requires more channel state information (CSI) to be available in the relays and also coordination of action between the relays. Consequently, opportunistic cooperation is not considered in this paper.

To clarify the motivation of this paper, we now give two definitions.

Definition I: In a cooperative network, a user's transmission freedom is defined as the ratio of the broadcasting transmission resource employed by a user in a particular cooperative scheme to that employed in a noncooperative scheme.

From this definition, it is shown that each user will have to sacrifice its usage of the channel, allowing others to relay its signal. User cooperation introduces a diversity gain; however, it will also result in a loss of transmission freedom, which can be interpreted as a loss of the achievable multiplexing gain [9], [15]. It is important to point out that later research on exploring the multiplexing gain by releasing the orthogonal constraint

Manuscript received November 3, 2010; revised February 23, 2011, April 11, 2011, and June 1, 2011; accepted June 29, 2011. Date of publication July 22, 2011; date of current version September 19, 2011. This work was supported in part by the U.K. Engineering and Physical Science Research Council under Grant EP/E012108/1 and in part by the National Natural Science Foundation of China under Grant 61001094. The review of this paper was coordinated by Dr. D. W. Matolak.

L. Chen is with the School of Information Science and Technology, Sun Yat-sen University, Guangzhou 510006, China (e-mail: chenli55@mail.sysu.edu.cn).

R. Carrasco is with the School of Electrical, Electronic and Computer Engineering, Newcastle University, Newcastle upon Tyne NE1 7RU, U.K. (e-mail: r.carrasco@ncl.ac.uk).

I. Wassell is with the Digital Technology Group, Computer Laboratory, University of Cambridge, Cambridge CB3 0FD, U.K. (e-mail: ijw24@cam.ac.uk).

Digital Object Identifier 10.1109/TVT.2011.2162756

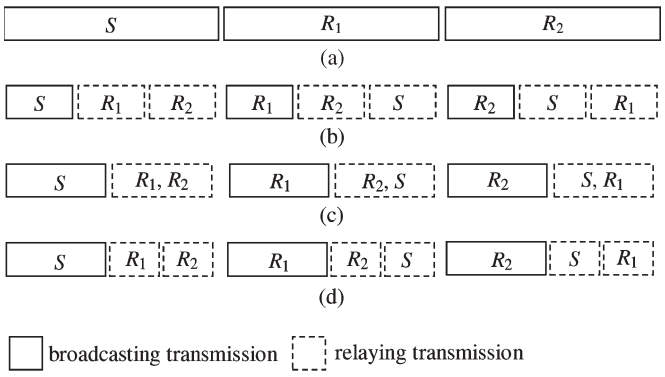

Fig. 1. Channel usage of different distributed cooperative schemes. (a) noncooperation. (b) RDAF cooperation. (c) STC cooperation. (d) MPDAF cooperation.

between broadcasting transmission and relaying transmission has been proposed in [9], [10], and [16]. However, releasing the orthogonal constraint is beyond the scope of our paper. This is due to two reasons. First, time orthogonal transmission is a common assumption in most of the multiuser systems. Second, we intend to maintain not only the transmission freedom but also the user spectral efficiency. For generality, we apply the orthogonal constraint for this paper.

Definition II: In a cooperative network, a user's spectral efficiency is defined as the number of its own information bits carried by each of its transmitted symbols. It is denoted by Γ.

In cooperative communications, one user will transmit its own information during broadcasting transmission while transmitting others' information during relaying transmission. Clearly, this will potentially lower the spectral efficiency of each user. We denote the number of one's own symbols transmitted in the broadcast interval and the number of symbols transmitted in the relay interval by $\mathcal{S}_{\rm BT}$ and $\mathcal{S}_{\rm RT}$, respectively. In a coded cooperative system that employs an error-correction code of rate θ and a modulation scheme of order m (e.g., $m = 2$ for quadrature phase-shift keying (QPSK) and $m = 4$ for 16-quadrature-amplitude modulation), the user spectral efficiency can be determined by

$$\Gamma = \frac{\theta m \mathcal{S}_{\rm BT}}{\mathcal{S}_{\rm BT} + \mathcal{S}_{\rm RT}} \text{ bits/symbol.} \tag{1}$$

Note that, in the case of noncooperation, $\mathcal{S}_{\rm RT} = 0$, and thus, $\Gamma = \theta m$ bits/symbol. However, user cooperation enforces $\mathcal{S}_{\rm RT} \neq 0$ and results in a loss of spectral efficiency. This problem was first addressed in [17] and [18] by using trellis-coded and high-order modulation schemes to compensate for the loss.

Fig. 1(a)–(c) shows the usage of a time orthogonal channel in noncooperation, RDAF cooperation, and STC cooperation, respectively, for a network of three users (S, R_1, and R_2). Notice that each user operates with the half-duplex constraint. In RDAF cooperation, each user can only use one third of their transmission compared with that for noncooperation for its own broadcasting, leaving two thirds available for relaying. Consequently, its achievable multiplexing gain is decreased to one third. The multiplexing gain will be further decreased as more cooperative users are involved. Therefore, while maintaining a certain transmission rate, the RDAF scheme cannot always provide a performance enhancement by simply increasing the number of relays. This issue is confirmed by the outage probability results in [8]. For STC cooperation, a user can always use half of its transmission compared with that for noncooperation for broadcasting its own data. Hence, increasing the number of cooperative users will not affect the achievable multiplexing gain, and performance can be enhanced. However, since STC cooperation is performed using the DF mode that necessitates decoding and encoding at the relays, its performance enhancement is at a significant cost in terms of system complexity. From the aspect of spectral efficiency, both RDAF and STC schemes have $\mathcal{S}_{\rm RT} = N\mathcal{S}_{\rm BT}$, and N is the total number of relays in the network, giving $\Gamma = \theta m/(N+1)$. Therefore, for both of these schemes, distributed cooperation is at the cost of reduced user spectral efficiency.

Based on these arguments, it is desirable to have a distributed cooperative scheme that can maintain both the transmission freedom and the user spectral efficiency while at the same time having low implementation complexity. The proposed message partitioning-based distributed AF (MPDAF) cooperative scheme achieves this by partitioning the transmitted message into several equal parts, each of which is relayed by a different user in the network. The channel usage of an MPDAF scheme with three cooperative users is indicated in Fig. 1(d), where it is shown that each user always maintains half of its transmission for broadcasting, keeping a constant transmission freedom regardless of the number of relays. Due to the fact that each user only retransmits parts of others' signal, the MPDAF scheme yields $\mathcal{S}_{\rm BT} = \mathcal{S}_{\rm RT}$ and has spectral efficiency that is always maintained at $\Gamma = \theta m/2$. Hence, it has better spectral efficiency than the existing RDAF and STC schemes. Since relays only retransmit the message using the AF mode, it has system complexity that is lower than that of the STC scheme. However, extra effort is required concerning the medium-access control (MAC) layer signal format to enable both signal recognition and user time synchronization. To validate the advantage of the MPDAF scheme, we investigate its performance from both information theoretic and practical communication system aspects. We first analyze the diversity–multiplexing tradeoff (DMT) characteristics of the MPDAF scheme, which quantifies the balance between the achievable diversity gain and the multiplexing gain. It is proved that the proposed scheme can achieve further diversity gain without affecting its multiplexing gain. This DMT analysis is supported by our numerical results in terms of the outage probability. We then analyze the impact of the proposed MPDAF scheme on a coded communication system by deriving the achievable diversity gain. Finally, we propose a coded cooperative system that combines the spectral efficient bit-interleaved coded modulation (BICM) with the proposed MPDAF scheme, aiming to validate the theoretical analysis. Earlier results from the research conducted in this area were presented by the authors in [19] and [20]. Compared with the previous work, this paper provides a consolidated analysis by theoretically validating the achievable diversity gain of a coded system [19] and proving that the DMT upper bound shown in [20] can be achieved.

The rest of this paper is organized as follows. Section II presents the preliminaries for this paper. Section III presents

the system model of the MPDAF scheme. Section IV presents the DMT analysis of the scheme. Section V investigates the impact of the proposed scheme on a practical coded system and proposes a BICM-coded MPDAF system. Finally, Section VI concludes this paper.

II. Preliminary

This section presents the preliminaries and defines the parameters that are used throughout this paper.

To simplify our analysis, the cooperative network is assumed to be symmetric, i.e., each channel has a similar quality, as measured by its signal-to-noise ratio (SNR), i.e.,

$$\rho = \frac{\varepsilon}{\sigma^2} \tag{2}$$

where ε denotes the average transmitted symbol energy for all users. It is a normalized value as $\varepsilon = 1$, and σ^2 denotes the variance of noise at the receiver. All the channels of the cooperative network are assumed to exhibit quasi-static Rayleigh fading and are statistically independent, where fading coefficient α is a complex Gaussian random variable with zero mean and unit variance. The function $1/|\alpha|^2$ has an exponential order of δ as defined in [9]

$$\delta = -\lim_{\rho\to\infty} \frac{\log\left(|\alpha|^2\right)}{\log \rho} \tag{3}$$

where the base of the logarithm is 2. Equation (3) can be alternatively written as $|\alpha|^2 \doteq \rho^{-\delta}$. Note that $\dot{\leq}$ and $\dot{\geq}$ are similarly defined. If $\delta \geq 0$, its probability density function can be written as [9]

$$p_\delta \doteq \rho^{-\delta}. \tag{4}$$

Definition III: Consider a coded system operating at an SNR of ρ, achieving a maximum-likelihood (ML) error probability of $P_E(\rho)$ and an average transmission rate of $R(\rho)$ bits/s/Hz. Its diversity gain d and multiplexing gain r are defined as [15]

$$d = -\lim_{\rho\to\infty} \frac{\log\left(P_E(\rho)\right)}{\log \rho}, \quad r = \lim_{\rho\to\infty} \frac{R(\rho)}{\log \rho}. \tag{5}$$

The derived relationship between d and r is known as the DMT, which is denoted by $d(r)$.

Let $\Re^N$ and $\Re^{N+}$ denote the set of N real tuples and the set of N nonnegative real tuples, respectively, and $\mathcal{C}^N$ denote the set of N complex tuples. Now, $\mathbf{O}$ denotes the set of outage events, and its complementary set (set of nonoutage events) is $\mathbf{O}^c$, where $\mathbf{O} \subseteq \Re^N$, $\mathbf{O}^c \subseteq \Re^N$, $\mathbf{O}^+ = \mathbf{O} \cap \Re^{N+}$, and $\mathbf{O}^{c+} = \mathbf{O}^c \cap \Re^{N+}$. The DMT (i.e., $d(r)$) of a cooperative system with N relays is upper bounded by [9], [15]

$$d(r) \leq d_0, \qquad d_0 = \inf_{(\delta_0,\delta_1,\ldots,\delta_N)\in\mathbf{O}^+} \sum_{j=0}^{N} \delta_j. \tag{16}$$

The probability P_O that the set of channel exponential orders $(\delta_0, \delta_1, \ldots, \delta_N)$ belongs to the set of outage events $\mathbf{O}$ is given by $P_O \doteq \rho^{-d_0}$.

Remark: For protocols A and B, if $d_{\mathrm{A}}(r) \geq d_{\mathrm{B}}(r)$ for all r, it can be claimed that protocol A is superior to protocol B. In other words, protocol A has an outage performance gain over protocol B.

For a coherent linear Gaussian channel $\boldsymbol{y} = \boldsymbol{s} + \boldsymbol{n}$, where $\boldsymbol{y} \in \mathcal{C}^N$ is the observed vector that consists of a signal component $\boldsymbol{s} \in \mathcal{C}^N$ and a noise component $\boldsymbol{n} \in \mathcal{C}^N$. Averaging over the ensemble of random Gaussian codes, the pairwise error probability of an ML decoder is upper bounded by

$$P_{PE} \leq \det\left(\mathbf{I}_N + \frac{1}{2}\Sigma_{\boldsymbol{s}}\Sigma_{\boldsymbol{n}}^{-1}\right)^{-1} \tag{17}$$

where $\mathbf{I}_N$ denotes the $N \times N$ identity matrix, and $\Sigma_{\boldsymbol{s}}$ and $\Sigma_{\boldsymbol{n}}$ are the autocovariance matrices of vectors $\boldsymbol{s}$ and $\boldsymbol{n}$, respectively. For a matrix $\mathbf{M}$, $\det(\mathbf{M})$, $\mathbf{M}^H$, and $\mathbf{M}^{-1}$ denote its determinant, Hermitian conjugate, and inverse, respectively. In addition, $(u)^+ = \max\{u, 0\}$, and $(u)^- = \min\{u, 0\}$.

III. System Model

This section presents descriptions for the MPDAF scheme at both the physical and the MAC layers. In general, if an MPDAF cooperative network has N relays, the transmitted signal of S will be partitioned into N equal frames, each of which will be relayed by a partner to D. For simplicity, the description of the MPDAF system model is given for $N = 2$, although it can be straightforwardly extended to a larger cooperative network.

A. Physical-Layer Signal Model

A complete cooperation process consists of two TSs, i.e., TS-I for S to broadcast its message and TS-II for relays to retransmit S's message. Before transmission, the transmitted message of S is partitioned into two equal parts, as shown in Fig. 2(a), where l denotes the length of S's message. In TS-I, S transmits both parts of its message to D. Assuming R_1 and R_2 are perfectly synchronized with S, R_1 receives the first half of S's message, whereas R_2 receives the second half. They will then take turns to retransmit an amplified version of their received message to D in TS-II. In the cooperative network, α_0, α_1, and α_2 denote the fading coefficients of the $S-D$, R_1-D, and R_2-D uplink channels, respectively, whereas γ_1 and γ_2 denote the fading coefficients of the $S-R_1$ and $S-R_2$ interuser channels, respectively. This is indicated in Fig. 2(b).

In the following description, x denotes the transmitted symbol, and y_{I} and y_{II} denote the received symbols of the two TSs. v, w_1, and w_2 are the additive white Gaussian noise (AWGN) components observed at D, R_1, and R_2, respectively. They are modeled as zero-mean mutually independent complex random sequences with variances σ_v^2, $\sigma_{w_1}^2$, and $\sigma_{w_2}^2$, respectively. The $S-D$ transmission in TS-I can be described as

$$y_{\mathrm{I}}[k] = \alpha_0 x[k] + v[k], \qquad k = 1, \ldots, l. \tag{8}$$

In addition, in TS-I, R_1 receives the first half of S's transmission, and R_2 receives the second half.

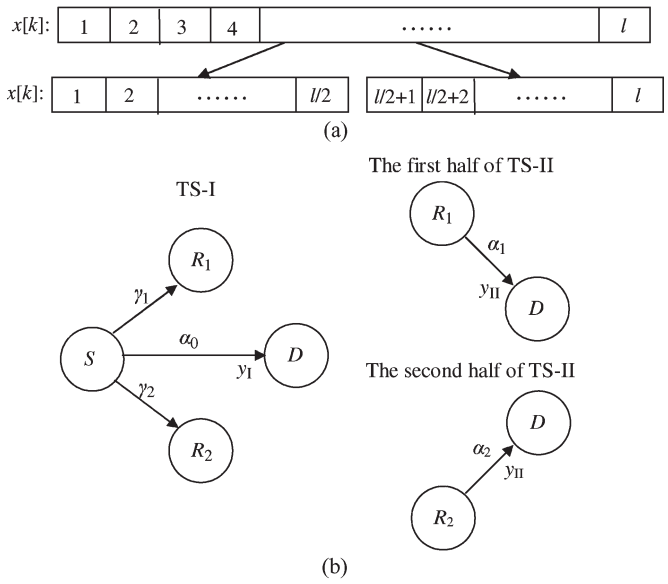

Fig. 2. Cooperation process of the MPDAF scheme. (a) Message partitioning. (b) Distributed cooperation.

TS-II is partitioned into two equal halves for relaying transmission. In the first half, R_1 amplifies its received signal with gain β_1 and retransmits to D as [4]

$$y_{\mathrm{II}}[k] = \alpha_1\beta_1\left(\gamma_1 x[k] + w_1[k]\right) + v[k+l], \quad k = 1, \ldots, l/2. \tag{9}$$

Similarly, in the second half, R_2 retransmits S's signal to D, i.e.,

$$y_{\mathrm{II}}[k] = \alpha_2\beta_2\left(\gamma_2 x[k] + w_2[k]\right) + v[k+l], \quad k = l/2+1, \ldots, l. \tag{10}$$

In (9) and (10), the amplification gain is [4]

$$\beta_t \le \sqrt{\frac{\varepsilon}{|\gamma_t|^2\varepsilon + \sigma_{w_t}^2}}, \qquad t = 1, 2. \tag{11}$$

After the two TSs, user D employs the ML combiner [5], [19] for combining $y_{\mathrm{I}}[k]$ with $y_{\mathrm{II}}[k]$, yielding the recovered sequence $y[k]$ $(k = 1, 2, \ldots, l)$. Decoding will be undertaken to retrieve the transmitted information. It is assumed that D has perfect CSI about the network.

B. MAC-Layer Signal Format

Acknowledging that the implementation of the MPDAF scheme is based on the assumption of perfect synchronization between all users, it is necessary to show a practical MAC-layer signal format and to indicate how the proposed physical-layer implementation can be realized.

The proposed MAC-layer signal format is based on the standard IEEE 802.11 structure [21] and its extension to the wireless cooperative network [22]. The MAC-layer frame transmission sequence of the MPDAF scheme is shown in Fig. 3. Prior to the data transmission, a handshaking process is required to initiate cooperation. S sends the ready-to-send (RTS) frame to D, R_1, and R_2. D then replies with a clear-to-send (CTS) frame to S, R_1, and R_2. Finally, R_1 and R_2 take turns replying

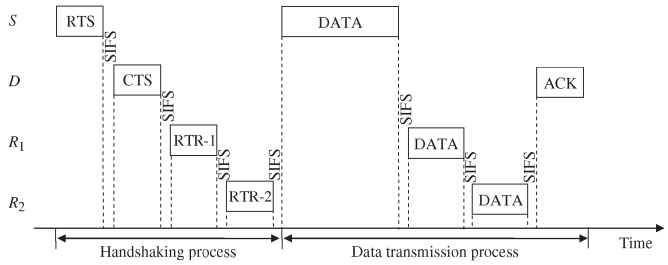

Fig. 3. Frame transmission sequence for the MPDAF scheme.

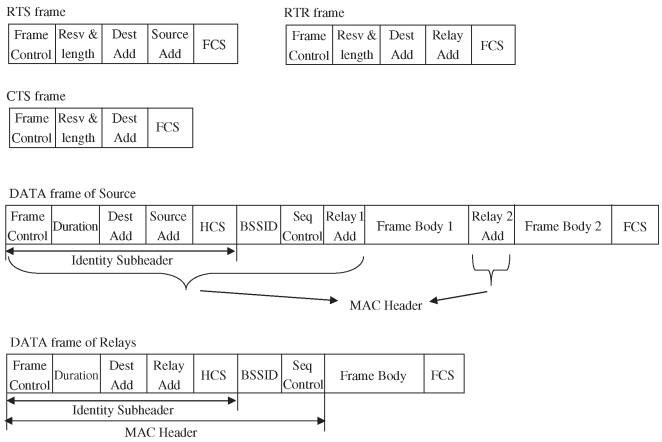

Fig. 4. MAC-layer frame format for the MPDAF scheme.

with a ready-to-relay (RTR) frame to both S and D. It is assumed that a coordination agreement has been reached between R_1 and R_2 for the order of reaction and retransmission. Notice that a short interframe space (SIFS) exists between the frames. The handshaking process also enables both channel and storage reservation. In the meantime, the CSI of the interuser channels is obtained at the relays, and the CSI of both the interuser and uplink channels is obtained at D. Data transmission from S and retransmissions from the relays will then take place over orthogonal TSs. Upon receiving the DATA frame from R_2, D will send out an acknowledgement (ACK) frame to S, R_1, and R_2, acknowledging the successful receipt of all the frames and canceling all the channel reservations.

To clarify the realization of message partitioning relaying and user synchronization, Fig. 4 shows the MAC-layer frame format for the RTS, CTS, RTR, and DATA frames. Each of the frames is encapsulated by the frame control sequence and the frame check sequence (FCS) to identify the type of the frame and the end of the frame, respectively. The frames also contain the addresses of the sender and the receiver. In the RTS frame, a subfield is used to reserve the channel and the memory requirement at D and the relays for storing the received signal. For example, according to the MPDAF physical-layer signal model that was previously described, a memory of l symbols is reserved at D, and a memory of $l/2$ symbols is reserved at the relays. The RTR frames also contain a similar subfield indicating the memory requirement at D. For the DATA frames, the frame body carries the intended message, whereas the MAC header carries other necessary identity and network information. Within the MAC header, an identity subheader containing the addresses of the sender and the receiver, the duration of

the frame, and the header check sequence (HCS) to enable confirmation of correct reception of the identity information is included. The basic service set identification (BSSID) and sequence control are used for network identification and duplicated frame detection, respectively. For the DATA frame of S, the frame body is partitioned into two equal halves, each of which begins with a relay address subfield. This relay address indicates which relay shall listen to the following frame body. At the same time, it also enables D to know how to combine the frame bodies of the DATA frames from S and the relays. After receiving the two DATA frames from the relays, D can perform ML combining by matching the relay addresses of the S's DATA frame and the relays' DATA frames. For example, frame bodies 1 and 2 are to be combined with the frame bodies sent by R_1 and R_2, respectively. Therefore, like most of the AF-type cooperative schemes, the MPDAF scheme has memory requirements at the relays to store the received symbols for retransmission, which is not the case for the STC scheme. Compared with the STC scheme, the advantage of the proposed scheme is that it does not need to perform decoding and reencoding of the data frames at the relays. However, it does require a more sophisticated MAC-layer signal format to enable signal recognition and user time synchronization.

IV. Diversity–Multiplexing Tradeoff

This section analyzes the DMT characteristics of the proposed scheme. It is achieved through modeling its outage behavior and then determining its asymptotic characteristics with $\rho \to \infty$. For both clarity and simplicity, we will again start by analyzing a scheme with two relays and then extend it to a general situation with an arbitrary number N $(N \geq 2)$ of relays.

A. Outage Behavior

To analyze the outage behavior of the MPDAF scheme, we will formalize the physical-layer signal model described in Section III-A into a matrix form. For $k = 1$ to $l/2$, we have

$$\begin{bmatrix} y_{\mathrm{I}}[k] \\ y_{\mathrm{II}}[k] \end{bmatrix} = \underbrace{\begin{bmatrix} \alpha_0 \\ \alpha_1\beta_1\gamma_1 \end{bmatrix}}_{\mathbf{G}_1} x[k] + \underbrace{\begin{bmatrix} 1 & 0 & 0 \\ 0 & \alpha_1\beta_1 & 1 \end{bmatrix}}_{\Upsilon_1} \underbrace{\begin{bmatrix} v[k] \\ w_1[k] \\ v[k+l] \end{bmatrix}}_{\mathbf{N}_1} \tag{12}$$

whereas for $k = l/2 + 1, \ldots, l$, we have

$$\begin{bmatrix} y_{\mathrm{I}}[k] \\ y_{\mathrm{II}}[k] \end{bmatrix} = \underbrace{\begin{bmatrix} \alpha_0 \\ \alpha_2\beta_2\gamma_2 \end{bmatrix}}_{\mathbf{G}_2} x[k] + \underbrace{\begin{bmatrix} 1 & 0 & 0 \\ 0 & \alpha_2\beta_2 & 1 \end{bmatrix}}_{\Upsilon_2} \underbrace{\begin{bmatrix} v[k] \\ w_2[k] \\ v[k+l] \end{bmatrix}}_{\mathbf{N}_2}. \tag{13}$$

The mutual information on the MPDAF scheme is

$$\mathcal{I} = \frac{l}{2} \sum_{t=1}^{2} \log\det\left[\mathbf{I}_2 + \varepsilon \mathbf{G}_t \mathbf{G}_t^H \left(\Upsilon_t \mathbb{E}\left[\mathbf{N}_t \mathbf{N}_t^H\right] \Upsilon_t^H\right)^{-1}\right] \tag{14}$$

where

$$\mathbf{G}_t \mathbf{G}_t^H = \begin{bmatrix} |\alpha_0|^2 & \alpha_0\alpha_t^*\beta_t\gamma_t^* \\ \alpha_0^*\alpha_t\beta_t\gamma_t & |\alpha_t|^2\beta_t^2|\gamma_t|^2 \end{bmatrix}$$

$$\Upsilon_t \mathbb{E}\left[\mathbf{N}_t \mathbf{N}_t^H\right] \Upsilon_t^H = \begin{bmatrix} \sigma_v^2 & 0 \\ 0 & \sigma_v^2 + |\alpha_t|^2\beta_t^2\sigma_{w_t}^2 \end{bmatrix}.$$

Substituting these results into (14) and performing a few algebraic manipulations, it can be determined that

$$\mathcal{I} = \frac{l}{2} \sum_{t=1}^{2} \log\left(1 + \frac{|\alpha_0|^2\varepsilon}{\sigma_v^2} + \frac{|\alpha_t|^2\beta_t^2|\gamma_t|^2\varepsilon}{\sigma_v^2 + |\alpha_t|^2\beta_t^2\sigma_{w_t}^2}\right). \tag{15}$$

When β_t meets the equality of (11) and in a symmetric network $(\varepsilon/\sigma_v^2) = (\varepsilon/\sigma_{w_1}^2) = (\varepsilon/\sigma_{w_2}^2) = \rho$, (15) can be simplified to

$$\mathcal{I} = \frac{l}{2} \sum_{t=1}^{2} \log\left(1 + |\alpha_0|^2\rho + f\left(|\alpha_t|^2\rho, |\gamma_t|^2\rho\right)\right) \tag{16}$$

where $f(\varpi, \varrho) = \varpi\varrho/(\varpi + \varrho + 1)$, and ϖ and ϱ are random variables.

If the MPDAF system achieves a transmission rate of R bits/s/Hz for two TSs, during which $2l$ symbols are transmitted, its outage probability is determined by

$$P_O = \Pr[\mathcal{I} < 2lR]. \tag{17}$$

By substituting (16) into (17), we can derive the outage probability of the MPDAF scheme as

$$P_O = \Pr\left[\prod_{t=1}^{2}\left(1 + |\alpha_0|^2\rho + f\left(|\alpha_t|^2\rho, |\gamma_t|^2\rho\right)\right) < 2^{4R}\right]. \tag{18}$$

Using the same methodology, these results can be generalized for an MPDAF system having an arbitrary number N $(N \geq 2)$ of relays as

$$P_O = \Pr\left[\prod_{t=1}^{N}\left(1 + |\alpha_0|^2\rho + f\left(|\alpha_t|^2\rho, |\gamma_t|^2\rho\right)\right) < 2^{2NR}\right]. \tag{19}$$

B. DMT

Building upon the outage probability model, this section will analyze the DMT characteristics of the scheme, aiming to reveal its advantages over the RDAF scheme in [8].

To determine a scheme's DMT performance, we shall determine both its upper and lower bounds. Since both d and r describe the system's asymptotic characteristics with $\rho \to \infty$, to analyze $d(r)$ for the proposed scheme, we shall also analyze the asymptotic behavior of mutual information $\mathcal{I}$. According to (6), the exponential orders of the fading coefficients define the

upper bound of the scheme's DMT performance. Based on (15), it is shown that

$$\lim_{\rho\to\infty}\frac{\mathcal{I}}{\log\rho} = \lim_{\rho\to\infty}\frac{l}{2\log\rho}\sum_{t=1}^{2}\log\left(1+|\alpha_0|^2\rho+\frac{|\alpha_t|^2\beta_t^2|\gamma_t|^2\rho}{1+|\alpha_t|^2\beta_t^2\sigma_{\omega_t}^2/\sigma_v^2}\right). \tag{20}$$

When $\rho\to\infty$, $|\alpha_0|^2\doteq\rho^{-\delta_{\alpha_0}}$, $|\alpha_t|^2\doteq\rho^{-\delta_{\alpha_t}}$, and $|\gamma_t|^2\doteq\rho^{-\delta_{\gamma_t}}$. Equation (11) indicates that $\beta_t^2\le 1/|\gamma_t|^2$, and hence, $\delta_{\beta_t}\le\delta_{\gamma_t}$. It is assumed that β_t is specifically chosen such that $\delta_{\beta_t}=(\delta_{\gamma_t})^-$. Under the condition of $(\delta_{\alpha_0},\delta_{\alpha_t},\delta_{\gamma_t}\ (t=1,2))\in\Re^{5+}$, $\delta_{\beta_t}=0$, and hence, $\beta_t^2\doteq 1$. Furthermore, under the symmetric condition, $\sigma_{\omega_t}^2/\sigma_v^2=1$. As a result, (20) simplifies to

$$\lim_{\rho\to\infty}\frac{\mathcal{I}}{\log\rho}=\frac{l\sum_{t=1}^{2}\log\left(1+\rho^{1-\delta_{\alpha_0}}+\rho^{1-(\delta_{\alpha_t}+\delta_{\gamma_t})}\right)}{2\log\rho}. \tag{21}$$

It can be further approximated as

$$\begin{aligned}\lim_{\rho\to\infty}\frac{\mathcal{I}}{\log\rho}&\cong\frac{l}{2}\sum_{t=1}^{2}\left(\max\left\{\frac{\log\rho^{1-\delta_{\alpha_0}}}{\log\rho},\frac{\log\rho^{1-(\delta_{\alpha_t}+\delta_{\gamma_t})}}{\log\rho}\right\}\right)^{+}\\&=\frac{l}{2}\sum_{t=1}^{2}\left(\max\left\{1-\delta_{\alpha_0},1-(\delta_{\alpha_t}+\delta_{\gamma_t})\right\}\right)^{+}.\end{aligned} \tag{22}$$

Equation (22) links the mutual information with the exponential order of each channel. The set of outage events is defined as the set of instantaneous channel realizations in which its mutual information falls below its transmission rate, i.e.,

$$\mathbf{O}=\left\{(\delta_{\alpha_0},\delta_{\alpha_t},\delta_{\gamma_t}\ (t=1,2))\mid\mathcal{I}<2lR)\right\}. \tag{23}$$

Based on (22) and knowing $R\doteq r\log\rho$, we can further define

$$\mathbf{O}^{+}=v\left\{(\delta_{\alpha_0},\delta_{\alpha_t},\delta_{\gamma_t}\ (t=1,2))\in\Re^{5+}\ \middle|\ \sum_{t=1}^{2}\left(\max\left\{1-\delta_{\alpha_0},1-(\delta_{\alpha_t}+\delta_{\gamma_t})\right\}\right)^{+}<4r\right\}. \tag{24}$$

According to (6), the DMT upper bound of the MPDAF ($N=2$) scheme can be derived as

$$d_0(r)=(1-2r)^{+}+(2-4r)^{+}=3(1-2r)^{+} \tag{25}$$

which also defines the lower bound of error probability as $P_E(\rho)\dot{\ge}P_O\doteq\rho^{-d_0(r)}$ [15]. Now, we have to determine the upper bound of $P_E(\rho)$, through which the lower bound of the scheme's DMT performance can be defined.

Let $P_{E,O}$ and P_{E,O^c} denote the error probabilities under the outage and nonoutage events, respectively. Now, $P_{E|O}$ denotes the conditional error probability under the outage events, and $P_E(\rho)$ can be upper bounded by

$$P_E(\rho)=P_{E,O}+P_{E,O^c}=P_{E|O}P_O+P_{E,O^c}\le P_O+P_{E,O^c}. \tag{26}$$

The conditional averaged pairwise error probability of the scheme is determined by

$$\begin{aligned}P_{PE|\alpha_0,\alpha_t,\gamma_t\ (t=1,2)}&=P_{PE|\alpha_0,\alpha_1,\gamma_1}\cdot P_{PE|\alpha_0,\alpha_2,\gamma_2}\\&\le\prod_{t=1}^{2}\det\left(\mathbf{I}_2+\frac{1}{2}\Sigma_{\boldsymbol{s}_t}\Sigma_{\boldsymbol{n}_t}^{-1}\right)^{-l/2}\end{aligned} \tag{27}$$

where

$$\Sigma_{\boldsymbol{s}_t}=\begin{bmatrix}|\alpha_0|^2 & \alpha_0\alpha_t^*\beta_t\gamma_t^*\\ \alpha_0^*\alpha_t\beta_t\gamma_t & |\alpha_t|^2\beta_t^2|\gamma_t|^2\end{bmatrix}\varepsilon \tag{28}$$

$$\Sigma_{\boldsymbol{n}_t}=\begin{bmatrix}\sigma_v^2 & 0\\ 0 & \sigma_v^2+|\alpha_t|^2\beta_t^2\sigma_{w_t}^2\end{bmatrix}. \tag{29}$$

Therefore

$$P_{PE|\alpha_0,\alpha_t,\gamma_t\ (t=1,2)}\le\prod_{t=1}^{2}\left[1+\frac{|\alpha_0|^2\varepsilon}{2\sigma_v^2}+\frac{|\alpha_t|^2\beta_t^2|\gamma_t|^2\varepsilon}{2\left(\sigma_v^2+|\alpha_t|^2\beta_t^2\sigma_{w_t}^2\right)}\right]^{-l/2}. \tag{30}$$

Its asymptotic behavior can be derived as

$$\lim_{\rho\to\infty}\frac{\log P_{PE|\delta_{\alpha_0},\delta_{\alpha_t},\delta_{\gamma_t}\ (t=1,2)}}{\log\rho}\le-\frac{l}{2}\sum_{t=1}^{2}\left(\max\left\{1-\delta_{\alpha_0},1-(\delta_{\alpha_t}+\delta_{\gamma_t})\right\}\right)^{+}. \tag{31}$$

or alternatively

$$P_{PE|\delta_{\alpha_0},\delta_{\alpha_t},\delta_{\gamma_t}(t=1,2)}\dot{\le}\rho^{-\frac{l}{2}\sum_{t=1}^{2}\left(\max\left\{1-\delta_{\alpha_0},1-(\delta_{\alpha_t}+\delta_{\gamma_t})\right\}\right)^{+}}. \tag{32}$$

Transmitting $2l$ symbols at a rate of $R=r\log(\rho)$, the total number of possible codewords is ρ^{2rl}. The conditional error probability can therefore be determined by

$$P_{E|\delta_{\alpha_0},\delta_{\alpha_t},\delta_{\gamma_t}\ (t=1,2)}=P_{PE|\delta_{\alpha_0},\delta_{\alpha_t},\delta_{\gamma_t}\ (t=1,2)}\cdot\rho^{2rl} \tag{33}$$

and hence

$$P_{E|\delta_{\alpha_0},\delta_{\alpha_t},\delta_{\gamma_t}\ (t=1,2)}\dot{\le}\rho^{-\frac{l}{2}\left[\sum_{t=1}^{2}\left(\max\left\{1-\delta_{\alpha_0},1-(\delta_{\alpha_t}+\delta_{\gamma_t})\right\}\right)^{+}-4r\right]}. \tag{34}$$

According to (4), with $(\delta_{\alpha_0},\delta_{\alpha_t},\delta_{\gamma_t}\ (t=1,2))\in\Re^{5+}$ and $\rho\to\infty$, we have P_{E,O^c} upper bounded as

$$\begin{aligned}P_{E,O^c}&=\int_{\mathbf{O}^{c+}}P_{E|\delta_{\alpha_0},\delta_{\alpha_t},\delta_{\gamma_t}\ (t=1,2)}\\&\quad\cdot\rho^{-\delta_{\alpha_0}-\delta_{\alpha_1}-\delta_{\alpha_2}-\delta_{\gamma_1}-\delta_{\gamma_2}}d\delta_{\alpha_0}d\delta_{\alpha_1}d\delta_{\alpha_2}d\delta_{\gamma_1}d\delta_{\gamma_2}\\&\dot{\le}\int_{\mathbf{O}^{c+}}\rho^{-d_e(r)}d\delta_{\alpha_0}d\delta_{\alpha_1}d\delta_{\alpha_2}d\delta_{\gamma_1}d\delta_{\gamma_2}.\end{aligned} \tag{35}$$

and

$$d_e(r)=\frac{l}{2}\left[\sum_{t=1}^{2}\left(\max\left\{1-\delta_{\alpha_0},1-(\delta_{\alpha_t}+\delta_{\gamma_t})\right\}\right)^{+}-4r\right]+\delta_{\alpha_0}+\delta_{\alpha_1}+\delta_{\alpha_2}+\delta_{\gamma_1}+\delta_{\gamma_2}. \tag{36}$$

Since P_{E,O^c} is dominated by the minimum value of $d_e(r)$, if we let

$$d'_e(r) = \inf_{\left(\delta_{\alpha_0},\delta_{\alpha_t},\delta_{\gamma_t}\ (t=1,2)\right)\in\mathbf{O}^{c+}} d_e(r) \tag{37}$$

then

$$P_{E,O^c} \dot{\leq} \rho^{-d'_e(r)}. \tag{38}$$

Based on (24), the complementary set of $\mathbf{O}^+$ is given as

$$\mathbf{O}^{c+} = \left\{ (\delta_{\alpha_0}, \delta_{\alpha_t}, \delta_{\gamma_t}\ (t=1,2)) \in \Re^{5+} \right.$$
$$\left. \left| \sum_{t=1}^{2} (\max\{1-\delta_{\alpha_0}, 1-(\delta_{\alpha_t}+\delta_{\gamma_t})\})^+ \geq 4r \right. \right\} \tag{39}$$

indicating in (36) that $(l/2)[\sum_{t=1}^{2}(\max\{1-\delta_{\alpha_0}, 1-(\delta_{\alpha_t}+\delta_{\gamma_t})\})^+ - 4r] \geq 0$. Based on the definition of $d_0(r)$, we know

$$d_0(r) = \inf_{\left(\delta_{\alpha_0},\delta_{\alpha_t},\delta_{\gamma_t}\ (t=1,2)\right)\in\mathbf{O}^{+}} (\delta_{\alpha_0}+\delta_{\alpha_1}+\delta_{\alpha_2}+\delta_{\gamma_1}+\delta_{\gamma_2})$$

and hence

$$d'_e(r) \geq d_0(r). \tag{40}$$

As a result

$$P_{E,O^c} \dot{\leq} P_O \tag{41}$$

which indicates that the $P_E(\rho)$ upper bound defined by (26) can be further simplified as

$$P_E(\rho) \dot{\leq} P_O. \tag{42}$$

Therefore, $d_0(r)$ of (25) is also a DMT lower bound of the MPDAF scheme. In conclusion, the DMT performance of the MPDAF scheme with $N = 2$ is characterized by

$$d(r) = 3(1-2r)^+. \tag{43}$$

Following a similar methodology, it is straightforward to extend the aforementioned result to an MPDAF scheme with an arbitrary number N $(N \geq 2)$ of relays, giving

$$d(r) = (N+1)(1-2r)^+. \tag{44}$$

Equation (43) indicates that no matter how many relays are involved in the signal retransmission, a maximal multiplexing gain of 0.5 is always maintained. It is the best achievable multiplexing gain of a cooperative scheme with the orthogonal constraint. Its DMT performance is identical to the STC scheme in [8], revealing how one can achieve the DMT performance bound of the STC scheme without necessitating decoding and encoding at the relays. In contrast to the RDAF scheme in [8], the proposed scheme can achieve a diversity gain on the order of the number of relays without affecting the multiplexing gain.

Fig. 5 shows the DMT performance of the MPDAF $(N = 2)$ scheme. It can achieve a maximal diversity gain of 3 and a maximal multiplexing gain of 0.5. In comparison with the RDAF schemes, MPDAF $(N = 2)$ achieves the same maximal multiplexing gain as RDAF $(N = 1)$ and the same maximal diversity gain as RDAF $(N = 2)$. Overall, the DMT curve of MPDAF $(N = 2)$ lies above those of both RDAF $(N = 1)$ and RDAF $(N = 2)$. Recalling the *Remark* of Section II, consequently, we can expect that MPDAF $(N = 2)$ can outperform the RDAF schemes with $N = 1$ and 2. Fig. 6 substantiates this claim by showing the outage performance. The MPDAF scheme's outage probability is achieved by evaluating the probability model of (18), whereas the RDAF scheme's outage probability is obtained by the probability model in [4] and [8]. It is shown that the MPDAF scheme can significantly outperform the RDAF scheme. With the same number of relays $N = 2$, the MPDAF scheme achieves a larger performance gain over RDAF at the higher transmission rate of $R = 2$.

Fig. 7 shows the DMT performance of the MPDAF scheme with $N = 2{-}5$. It can be observed that, by increasing the number of relays, its maximal multiplexing gain remains unchanged, but its maximal diversity gain is accordingly increased. However, for the RDAF scheme, the additional diversity gain is created at the cost of reduced multiplexing gain. Since increasing N cannot provide a DMT improvement (losing the multiplexing gain), neither can it guarantee an outage performance improvement. Again, the outage performance in Fig. 8 substantiates the DMT characteristics shown in Fig. 7, showing that the MPDAF scheme can maintain a stable performance improvement as the number of relays is increased.

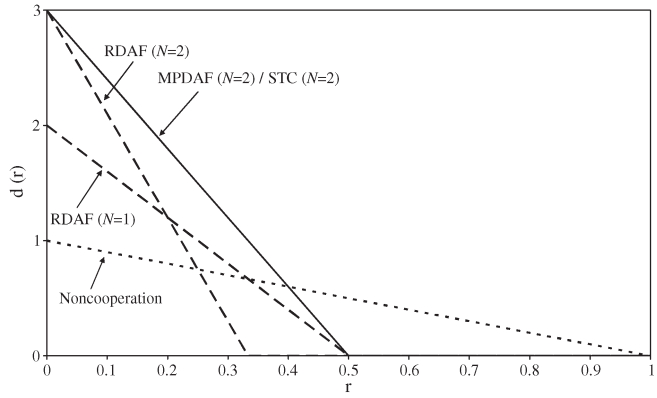

Fig. 5. DMT performance of the MPDAF scheme $(N = 2)$.

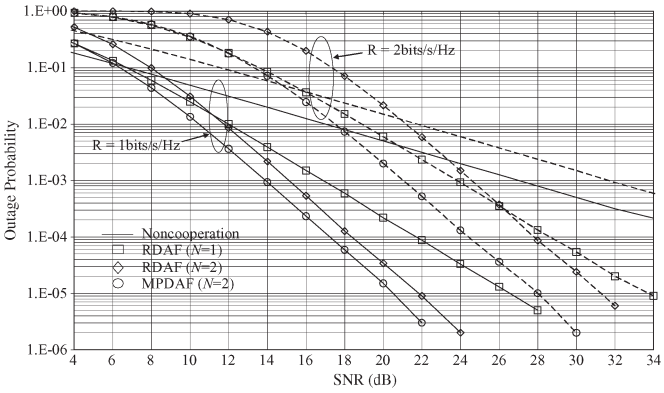

Fig. 6. Outage probability performance of the MPDAF scheme ($R =$ 1 bit/s/Hz and $R = 2$ bits/s/Hz).

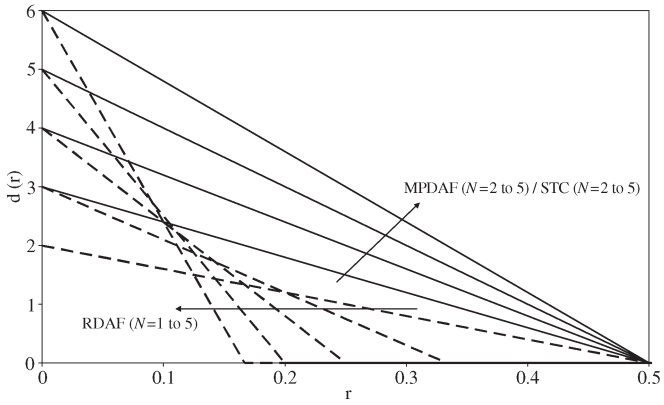

Fig. 7. DMT performance of the MPDAF scheme ($N = 2{-}5$).

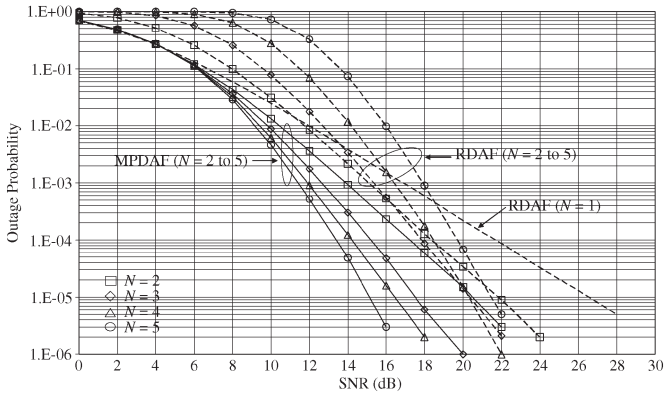

Fig. 8. Outage probability performance of the MPDAF scheme ($R =$ 1 bit/s/Hz and $N = 2{-}5$).

However, it is not the case for the RDAF scheme over the low-to-medium SNR region. These results reveal how to achieve a stable performance improvement in a large distributed network without the necessity of having to perform the DF operation in the relays.

It is worthwhile to mention that the outage probability and DMT performance conclusions are reached with the symmetric network assumption. However, the results we have obtained can be applied to a more realistic situation where each channel has a different SNR. For example, in (16), (18), and (19), one should only replace the common ρ value by a set of individual ρ values for the corresponding channels. Letting ρ_{α_0}, ρ_{α_t}, and ρ_{γ_t} denote the SNR values of the $S{-}D$, $R_t{-}D$, and $S{-}R_t$ channels, respectively, the outage probability (19) can be rewritten as

$$P_O = \Pr\left[\prod_{t=1}^{N}\left(1+|\alpha_0|^2\rho_{\alpha_0}+f\left(|\alpha_t|^2\rho_{\alpha_t},|\gamma_t|^2\rho_{\gamma_t}\right)\right)<2^{2NR}\right].$$

Since the DMT performance bound is derived from the asymptotic situation where $\rho \to \infty$, it will therefore remain unchanged when a realistic situation is concerned.

V. Impact on a Coded System

Based on the previous information theoretic analysis, this section will analyze the proposed scheme's impact on a practical coded system. The widely used trellis code is chosen for our investigation. Through analyzing the coded system's pairwise error probability, it is shown that the MPDAF scheme can indeed provide a full diversity gain for the coded system. Use of the BICM scheme is proposed for the MPDAF system, and our simulation results show that a significant diversity gain can be achieved for a coded system.

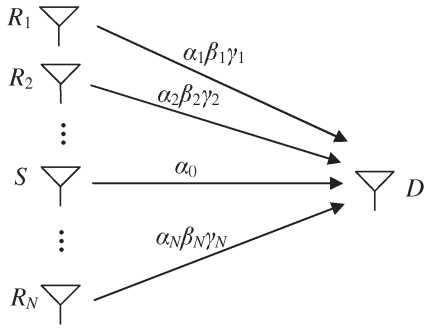

Fig. 9. Equivalent MISO channel model of the MPDAF scheme.

A. System Performance Assessment

This section will analyze the pairwise error probability for a coded MPDAF system. Since the cooperative system can be also interpreted as a multiple-input–single-output (MISO) system, a representation of the MPDAF system can be simplified into a MISO arrangement, as shown in Fig. 9. Equivalently, there are $N+1$ transmit antennas representing the antennas of S and R_i $(i = 1, \ldots, N)$ and one receive antenna representing the antenna of D. The $S{-}R{-}D$ channel gains can be equivalently expressed as $\alpha_1\beta_1\gamma_1, \alpha_2\beta_2\gamma_2, \ldots, \alpha_N\beta_N\gamma_N$. The $N+1$ antennas transmit through orthogonal TSs to avoid interuser interference; therefore, the performance assessment methodology of a MISO system [23] can be applied to analyze the proposed scheme.

For consistency, we are still considering a coded MPDAF system with two relays, i.e., $N = 2$. Based on the signal model of Section III, signal vector $\mathbf{x}$ is transmitted from S as

$$\mathbf{x} = \{x[1], x[2], \ldots, x[l/2], x[l/2+1], x[l/2+2], \ldots, x[l]\}.$$

Symbols $x[1], x[2], \ldots, x[l/2]$ are transmitted through the $S{-}D$ and $S{-}R_1{-}D$ channels, experiencing channel gains α_0 and $\alpha_1\beta_1\gamma_1$, respectively. Similarly, symbols $x[l/2+1], x[l/2+2], \ldots, x[l]$ experience channel gains of α_0 and $\alpha_2\beta_2\gamma_2$, respectively. Received vector $\mathbf{y}$ is

$$\mathbf{y} = \{y[1], y[2], \ldots, y[l/2], y[l/2+1], y[l/2+2], \ldots, y[l]\}.$$

By applying an ML decoder, it estimates an erroneous transmitted vector $\mathbf{e}$ as

$$\mathbf{e} = \{e[1], e[2], \ldots, e[l/2], e[l/2+1], e[l/2+2], \ldots, e[l]\}.$$

In a practical coded system, pairwise error probability $P(\mathbf{x} \to \mathbf{e})$ denotes the probability that the ML decoder output is in favor of $\mathbf{e}$ rather than $\mathbf{x}$. Notice that $P(\mathbf{x} \to \mathbf{e})$ is defined differently from the information theoretic pairwise error probability P_{PE}

that was defined in Section II. With the knowledge of network CSI, $P(\mathbf{x} \to \mathbf{e})$ can be approximately upper bounded by [23]

$$P\left(\mathbf{x} \to \mathbf{e} \mid \alpha_0, \alpha_t, \beta_t, \gamma_t \ (t = 1, 2)\right) \leq \exp\left(-d^2(\mathbf{x}, \mathbf{e})\rho/4\right) \tag{45}$$

where distance value $d^2(\mathbf{x}, \mathbf{e})$ is defined as

$$d^2(\mathbf{x}, \mathbf{e}) = |\alpha_0|^2 \sum_{k=1}^{l} |x[k] - e[k]|^2 + |\alpha_1\beta_1\gamma_1|^2 \sum_{k=1}^{l/2} |x[k]$$

$$-e[k]|^2 + |\alpha_2\beta_2\gamma_2|^2 \sum_{k=l/2+1}^{l} |x[k] - e[k]|^2 . \tag{46}$$

To analyze the diversity gain provided by the MPDAF scheme, we have to rewrite the expression of (45) in matrix form. Let us define a 1×3 matrix Ω as

$$\Omega = [\alpha_0 \quad \alpha_1\beta_1\gamma_1 \quad \alpha_2\beta_2\gamma_2] \tag{47}$$

and a 3×3 diagonal matrix Λ as (48), shown at the bottom of the page.

The pairwise error probability of (45) can be alternatively expressed as

$$P\left(\mathbf{x} \to \mathbf{e} \mid \alpha_0, \alpha_t, \beta_t, \gamma_t \ (t = 1, 2)\right) \leq \exp(-\Omega\Lambda\Omega^H\rho/4). \tag{49}$$

To calculate the averaged upper bound for $P(\mathbf{x} \to \mathbf{e})$, it is assumed that the interuser channels are noiseless so that $\sigma^2_{w_1} = \sigma^2_{w_2} = 0$ and β_t is a complex random variable satisfying $\beta_t = 1/\gamma_t$, yielding $\alpha_t\beta_t\gamma_t = \alpha_t$. Therefore, we can consider that the three component entries of Ω are all Rayleigh random variables. Consequently, the pairwise error probability upper bound of (49) can be averaged as [23]

$$P\left(\mathbf{x} \to \mathbf{e} \mid \alpha_0, \alpha_t, \beta_t, \gamma_t \ (t = 1, 2)\right) \leq \left[\prod_{i=1}^{\phi}(1 + \lambda_i\rho/4)\right]^{-1} \tag{50}$$

where λ_i is the eigenvalue of matrix Λ, and ϕ is the rank of matrix Λ as $\phi \leq 3$. Since the orthogonal time transmission between all the users will always result in a diagonal signal matrix Λ of size 3×3, we have $\phi = 3$. Therefore

$$P\left(\mathbf{x} \to \mathbf{e} \mid \alpha_0, \alpha_t, \beta_t, \gamma_t \ (t = 1, 2)\right) \leq \left[\prod_{i=1}^{3}(1 + \lambda_i\rho/4)\right]^{-1}$$

$$\leq \left(\prod_{i=1}^{3}\lambda_i\right)^{-1} (\rho/4)^{-3}. \tag{51}$$

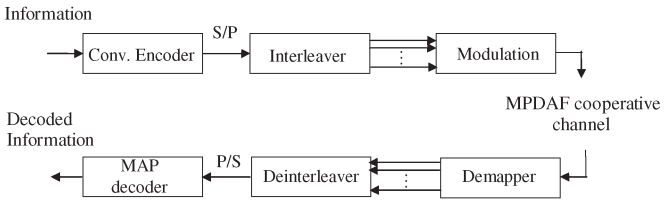

Fig. 10. BICM-coded MPDAF system.

From this equation, it is shown that a diversity gain of 3 can be achieved. At the same time, a coding advantage of $(\lambda_1\lambda_2\lambda_3)^{-1}$ is offered through the deployment of a code. The aforementioned analysis can be readily extended to a larger network with an arbitrary number of relays. Following a similar approach, the pairwise error probability for a coded MPDAF network with N relays is upper bounded by

$$P\left(\mathbf{x} \to \mathbf{e} \mid \alpha_0, \alpha_t, \beta_t, \gamma_t \ (t = 1, 2, \ldots, N)\right)$$

$$\leq \left(\prod_{i=1}^{N+1}\lambda_i\right)^{-1} (\rho/4)^{-(N+1)}. \tag{52}$$

It is important to mention that, since the established diversity gain is achieved based on the assumption of noiseless interuser channels, this is equivalent to assuming that the MPDAF cooperative network is functioning with genie-aided relays. With the help of a genie, the relays have exact knowledge of the transmitted symbols of S. They then take turns to forward parts of S's symbols to user D. Hence, better results will be achieved via this analysis compared with that achieved by a system without genies. However, through investigating the following simulation results of a BICM-coded system, it is shown that the achievable diversity gain will not be affected by this assumption.

B. System Design

Based on the previous analysis, this section considers the design of a coded MPDAF system using BICM [24], [25]. The BICM scheme can be spectrally efficient if high-order modulation schemes are used. More importantly, as indicated by earlier work in [19], for a trellis code to benefit from this distributed cooperation, it is important to introduce diversity into the trellis transition branches. The BICM scheme is capable of transferring the diversity effect into the trellis transition branches, thus enhancing the performance of the decoding algorithm. We will also present simulation results, comparing the performance of coded MPDAF and RDAF systems of the same spectral efficiency Γ.

Fig. 10 shows the design of a BICM-coded MPDAF system. Depending on the modulation scheme, the convolutional

$$\Lambda = \begin{bmatrix} \sum_{k=1}^{l} |x[k] - e[k]|^2 & 0 & 0 \\ 0 & \sum_{k=1}^{l/2} |x[k] - e[k]|^2 & 0 \\ 0 & 0 & \sum_{k=l/2+1}^{l} |x[k] - e[k]|^2 \end{bmatrix} \tag{48}$$

codeword is passed to the serial-to-parallel (S/P) converter generating m parallel codeword streams. The number of codeword streams is consistent with the order of the modulation scheme. The m codeword streams are then randomly interleaved before modulation. The modulated symbols $x[1], x[2], \ldots x[l]$ will be transmitted through the MPDAF channel. At the receiver, the received symbols $y[1], y[2], \ldots, y[l]$ will be passed to a demapper, generating *a posteriori* probability (APP) values for each of the coded bits. They are then deinterleaved and converted back to a serial probability stream by a parallel-to-serial (P/S) converter. The decoder will perform the maximum *a posteriori* (MAP) algorithm [26] to retrieve the information. Instead of focusing on trellis decoding [24]–[27], this paper will focus on revealing how the diversity effect of the MPDAF scheme is transferred into the trellis transition branches to assist error correction. We provide the following example to give a clearer indication.

Example: A rate 1/2 convolutional code and QPSK modulation are used in a BICM scheme, which is deployed in an MPDAF system with two relays. The following codeword is generated from the encoder:

$$c_1^1, c_1^2, c_2^1, c_2^2, c_3^1, c_3^2, c_4^1, c_4^2, c_5^1, c_5^2, c_6^1, c_6^2$$

where c_κ^b $(b = 1$ or $2)$ represents the two binary-coded bits generated at time κ $(\kappa = 1, 2, \ldots, 6)$ of the encoder. After S/P conversion, two streams of coded bits are generated as

$$c_1^1, c_2^1, c_3^1, c_4^1, c_5^1, c_6^1$$
$$c_1^2, c_2^2, c_3^2, c_4^2, c_5^2, c_6^2.$$

They are then randomly interleaved, yielding

$$c_3^1, c_1^1, c_2^1, c_6^1, c_4^1, c_5^1$$
$$c_5^2, c_4^2, c_2^2, c_3^2, c_6^2, c_1^2.$$

Now, (c_3^1, c_5^2), (c_1^1, c_4^2), (c_2^1, c_2^2), (c_6^1, c_3^2), (c_4^1, c_6^2), and (c_5^1, c_1^2) are grouped and mapped to QPSK symbols $x[1]$, $x[2]$, $x[3]$, $x[4]$, $x[5]$, and $x[6]$, respectively. They are then transmitted through the MPDAF $(N = 2)$ channel. The received symbols at D are $y[1]$, $y[2]$, $y[3]$, $y[4]$, $y[5]$, and $y[6]$, where symbols $y[1]$, $y[2]$, and $y[3]$ experience channel gains α_0 and $\alpha_1\beta_1\gamma_1$, and symbols $y[4]$, $y[5]$, and $y[6]$ experience channel gains α_0 and $\alpha_2\beta_2\gamma_2$. The demapper will then produce two streams of APP values $\Pr[c_\kappa^b = \vartheta \mid y[k]]$ representing the probability of coded bit c_κ^b being ϑ $(\vartheta = 0$ or $1)$, given the received symbol $y[k]$, as shown in (53), shown at the bottom of the page. After deinterleaving, the two streams of APP values are shown in (54), shown at the bottom of the page.

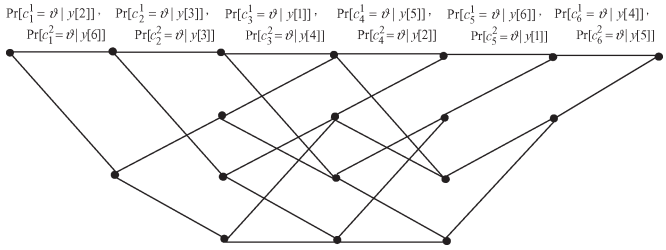

Fig. 11. Diversity reflected in a decoding trellis.

TABLE I
SYSTEM PARAMETERS OF THE BICM-CODED MPDAF SCHEME WITH $\Gamma = 0.5$ bit/symbol

Schemes	Code	Modulation	Spectral efficiency (Γ)
noncooperation	Conv $(15, 17)_8$	QPSK	1
RDAF $(N = 1)$		QPSK	0.5
RDAF $(N = 2)$		8PSK	0.5
MPDAF		QPSK	0.5

TABLE II
SYSTEM PARAMETERS OF THE BICM-CODED MPDAF SCHEME WITH $\Gamma = 1$ bit/symbol

Schemes	Code	Modulation	Spectral efficiency (Γ)
noncooperation	Conv $(15, 17)_8$	16QAM	2
RDAF $(N = 1)$		16QAM	1
RDAF $(N = 2)$		64QAM	1
MPDAF		16QAM	1

P/S conversion is performed on the deinterleaved APP values, generating a series of probability values that will be used in the following MAP decoding algorithm. Fig. 11 shows the diversity effect reflected in a trellis, where it is shown that each trellis transition branch produces two coded bits. Their APP values are used to calculate the state transition probabilities of the MAP algorithm [26]. Since most of the APP values of two coded bits are calculated with the knowledge of received symbols that are transmitted from different channels, diversity is introduced into the trellis transition branches. For example, $\Pr[c_1^1 = \vartheta | y[2]]$ and $\Pr[c_1^2 = \vartheta | y[6]]$ are calculated with the knowledge of $y[2]$ and $y[6]$ and their respective channels gains $\alpha_0, \alpha_1\beta_1\gamma_1$ and $\alpha_0, \alpha_2\beta_2\gamma_2$. The ability to introduce diversity into the trellis transition branches will enhance the performance of the decoding algorithm.

After investigating the diversity effect introduced by the MPDAF scheme, we propose two BICM-coded MPDAF systems with spectral efficiency values of $\Gamma = 0.5$ bit/symbol and $\Gamma = 1$ bit/symbol. They are to be compared with coded RDAF

$$\begin{array}{llllll} \Pr\left[c_3^1 = \vartheta | y[1]\right] & \Pr\left[c_1^1 = \vartheta | y[2]\right] & \Pr\left[c_2^1 = \vartheta | y[3]\right] & \Pr\left[c_6^1 = \vartheta | y[4]\right] & \Pr\left[c_4^1 = \vartheta | y[5]\right] & \Pr\left[c_5^1 = \vartheta | y[6]\right] \\ \Pr\left[c_5^2 = \vartheta | y[1]\right] & \Pr\left[c_4^2 = \vartheta | y[2]\right] & \Pr\left[c_2^2 = \vartheta | y[3]\right] & \Pr\left[c_3^2 = \vartheta | y[4]\right] & \Pr\left[c_6^2 = \vartheta | y[5]\right] & \Pr\left[c_1^2 = \vartheta | y[6]\right] \end{array} \quad (53)$$

$$\begin{array}{llllll} \Pr\left[c_1^1 = \vartheta | y[2]\right] & \Pr\left[c_2^1 = \vartheta | y[3]\right] & \Pr\left[c_3^1 = \vartheta | y[1]\right] & \Pr\left[c_4^1 = \vartheta | y[5]\right] & \Pr\left[c_5^1 = \vartheta | y[6]\right] & \Pr\left[c_6^1 = \vartheta | y[4]\right] \\ \Pr\left[c_1^2 = \vartheta | y[6]\right] & \Pr\left[c_2^2 = \vartheta | y[3]\right] & \Pr\left[c_3^2 = \vartheta | y[4]\right] & \Pr\left[c_4^2 = \vartheta | y[2]\right] & \Pr\left[c_5^2 = \vartheta | y[1]\right] & \Pr\left[c_6^2 = \vartheta | y[5]\right] \end{array} \quad (54)$$

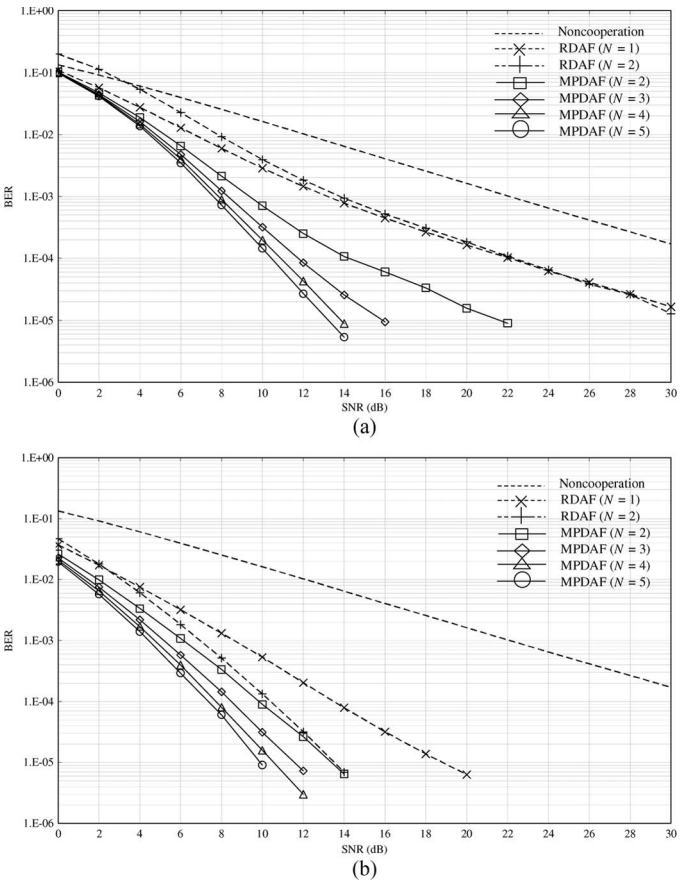

Fig. 12. BICM-coded MPDAF system with $\Gamma = 0.5$ bit/symbol. (a) Without genie-aided relays. (b) With genie-aided relays.

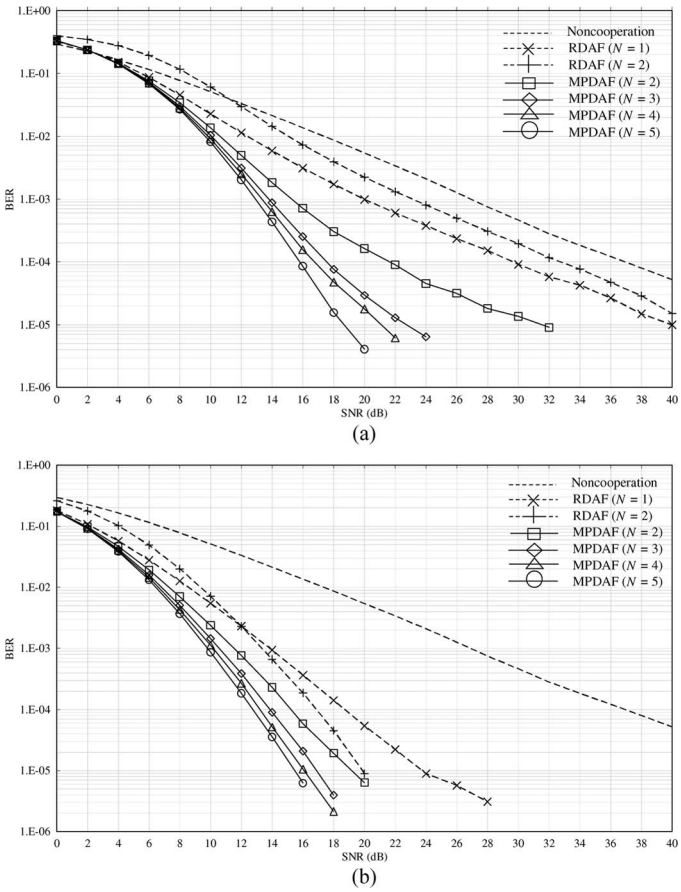

Fig. 13. BICM-coded MPDAF system with $\Gamma = 1$ bit/symbol. (a) Without genie-aided relays. (b) With genie-aided relays.

systems with one or two relays. According to Definition II, the MPDAF scheme can always achieve the same spectral efficiency as RDAF $(N = 1)$. However, for RDAF $(N = 2)$, $\mathcal{S}_{\mathrm{RT}} = 2\mathcal{S}_{\mathrm{BT}}$, one may have to raise the order of the modulation scheme to maintain the same spectral efficiency as the MPDAF scheme. The parameters of the two BICM-coded MPDAF systems are listed in Tables I and II, respectively. In both tables, it is important to notice that RDAF $(N = 2)$ has deployed a higher order modulation scheme to compensate for the spectral efficiency loss.

Figs. 12 and 13 show the bit-error-rate (BER) performance of the two coded systems, both with and without the assumption of genie-aided relays. The systems with genie-aided relays provide a better performance than the systems without genie-aided relays. More importantly, they both show that, with the same number of relays (e.g., $N = 2$), the coded MPDAF system achieves significant performance gains over the coded RDAF system. With the coded MPDAF system, a diversity gain on the order of the number of relays is achieved. They validate the system performance assessment given previously. However, for the coded RDAF system without genie-aided relays, RDAF $(N = 2)$ can barely outperform RDAF $(N = 1)$, particularly for systems with higher spectral efficiency. This is due to the fact that, to maintain the same spectral efficiency, RDAF $(N = 2)$ is forced to employ a higher order modulation scheme than RDAF $(N = 1)$. In the situation with genie-aided relays, performance degradation introduced by the use of a higher order modulation scheme is less significant. The coded RDAF $(N = 2)$ system is able to achieve a diversity gain over the coded RDAF $(N = 1)$ system. Our finding substantiates the information theoretic performances shown in Figs. 6 and 8. In both figures, it can be observed that, with a certain transmission rate, the RDAF scheme cannot provide a performance improvement by increasing the number of relays over the low-to-medium SNR region. It demonstrates the necessity to perform distributed AF cooperation with the assistance of message partitioning.

It is also worthwhile to mention that, by increasing the number of relays from two to three, one can achieve a substantially large performance gain. However, by increasing the number of relays to more than three, relatively less improvement can be made. A similar phenomenon can be also found out if we review the MPDAF scheme's outage performance presented in Fig. 8. These observations are consistent with the results in [28], which show that, for a MISO system, little improvement can be made by using more than four transmit antennas. According to Section III-B, it should be recalled that increasing the number of relays will raise the system complexity owing to the increasing demands of signal recognition, user synchronization, and signal combining. Therefore, our results show that MPDAF $(N = 3)$ offers the best performance–complexity tradeoff for a practical implementation.

VI. Conclusion

A distributed AF cooperative scheme achieved through message partitioning has been proposed. By performing message partitioning for distributed relaying, one cannot only introduce diversity into the transmitted message but also enable the cooperative users to share the relaying burden. The DMT analysis showed that the MPDAF scheme can always maintain its achievable multiplexing gain to 0.5 while achieving a diversity gain on the order of the number of relays. It is superior to the RDAF scheme and is identical to the STC scheme but has lower system complexity. We also noted that the MAC-layer frame format does need to be modified to enable the recognition of partitioned signals and for user time synchronization. The outage probability results showed that a significant performance gain can be achieved over an RDAF scheme having the same number of relays. Another advantage of message partitioning is to enable the cooperative users to maintain constant spectral efficiency that is half that of noncooperation. However, for both RDAF and STC schemes, spectral efficiency will be degraded by increasing the number of relays. Consequently, to maintain the spectral efficiency for those schemes, one will be forced to deploy a high-order modulation scheme or a high-rate code, thus affecting the system performance. We also investigated the performance of the MPDAF scheme in a practical coded system. This showed that the system diversity gain can be also achieved on the order of the number of relays. Use of the spectrally efficient BICM was proposed for the MPDAF scheme, revealing how a practical coded system can benefit from the proposed scheme. Our simulation results showed that, while maintaining the same spectral efficiency, the MPDAF scheme can significantly outperform the RDAF scheme. Therefore, this paper offers a good performance while having low complexity, thus making it suitable for practical cooperative applications.

References

[1] S. M. Alamouti, "A simple transmit diversity technique for wireless communications," *IEEE J. Sel. Areas Commun.*, vol. 16, no. 8, pp. 1451–1458, Oct. 1998.

[2] A. Sendonaris, E. Erkip, and B. Aazhang, "User cooperation diversity. Part I. System description," *IEEE Trans. Commun.*, vol. 51, no. 11, pp. 1927–1938, Nov. 2003.

[3] A. Sendonaris, E. Erkip, and B. Aazhang, "User cooperation diversity. Part II. Implementation aspects and performance analysis," *IEEE Trans. Commun*, vol. 51, no. 11, pp. 1939–1948, Nov. 2003.

[4] J. N. Laneman, D. N. C. Tse, and G. W. Wornell, "Cooperative diversity in wireless networks: Efficient protocols and outage behavior," *IEEE Trans. Inf. Theory*, vol. 50, no. 12, pp. 3062–3080, Dec. 2004.

[5] J. N. Laneman and G. W. Wornell, "Energy-efficient antenna sharing and relaying for wireless networks," in *Proc. IEEE Wireless Commun. Netw. Conf.*, Chicago, IL, 2000, pp. 7–12.

[6] T. E. Hunter and A. Nosratinia, "Diversity through coded cooperation," *IEEE Trans. Wireless Commun*, vol. 5, no. 2, pp. 283–289, Feb. 2006.

[7] A. Stefanov and E. Erkip, "Cooperative coding for wireless networks," *IEEE Trans. Commun*, vol. 52, no. 9, pp. 1470–1476, Sep. 2004.

[8] J. N. Laneman and G. W. Wornell, "Distributed space–time-coded protocols for exploiting cooperative diversity in wireless networks," *IEEE Trans. Inf. Theory*, vol. 49, no. 10, pp. 2415–2425, Oct. 2003.

[9] K. Azarian, H. El Gamal, and P. Schniter, "On the achievable diversity–multiplexing tradeoff in half-duplex cooperative channels," *IEEE Trans. Inf. Theory*, vol. 51, no. 12, pp. 4152–4172, Dec. 2005.

[10] S. Yang and J. C. Belfiore, "Towards the optimal amplify-and-forward cooperative diversity scheme," *IEEE Trans. Inf. Theory*, vol. 53, no. 9, pp. 3114–3126, Sep. 2007.

[11] A. Stefanov and E. Erkip, "Cooperative space–time coding for wireless networks," in *Proc. IEEE Inf. Theory Workshop*, Paris, France, 2003, pp. 50–53.

[12] M. Janani, A. Hedayat, T. Hunter, and A. Norsratinia, "Coded cooperation in wireless communications: Space–time transmission and iterative decoding," *IEEE Trans. Signal Process.*, vol. 52, no. 2, pp. 362–371, Feb. 2004.

[13] A. Bletsas, A. Khisti, D. Reed, and A. Lippman, "A simple cooperative diversity method based on network path selection," *IEEE J. Sel. Areas Commun.*, vol. 24, no. 3, pp. 659–672, Mar. 2006.

[14] A. Bletsas, H. Shin, and M. Win, "Cooperative communications with outage-optimal opportunistic relaying," *IEEE Trans. Wireless Commun.*, vol. 6, no. 9, pp. 3450–3460, Sep. 2007.

[15] L. Zheng and D. N. C. Tse, "Diversity and multiplexing: A fundamental tradeoff in multiple-antenna channels," *IEEE Trans. Inf. Theory*, vol. 49, no. 5, pp. 1073–1096, May 2003.

[16] R. U. Nabar, F. W. Kneubuhler, and H. Bolcskei, "Fading relay channels: Performance limits and space–time signal design," *IEEE J. Sel. Areas Commun.*, vol. 22, no. 6, pp. 1099–1109, Aug. 2004.

[17] L. Chen, R. A. Carrasco, S. LeGoff, and I. J. Wassell, "Cooperative amplify-and-forward with trellis coded modulation," in *Proc. IEEE Wireless Commun. Netw. Conf.*, Budapest, Hungary, 2009, pp. 1–5.

[18] I. Chatzigeorgiou, W. Guo, I. J. Wassell, and R. A. Carrasco, "Comparison of cooperative schemes using joint channel coding and high-order modulation," in *Proc. 3rd IEEE Int. Symp. Commun., Control Signal Process.*, St. Julians, Malta, Mar. 2008, pp. 994–998.

[19] L. Chen, R. Carrasco, and I. J. Wassell, "Distributed amplify-and-forward with ring-TCM codes," in *Proc. IEEE Consum. Commun. Netw. Conf.*, Las Vegas, NV, 2010, pp. 1–5.

[20] L. Chen, R. Carrasco, and I. J. Wassell, "Distributed amplify-and-forward cooperation with maintaining transmission freedom," in *Proc. IEEE/IET Int. Symp. Commun. Syst., Netw. Dig. Signal Process.*, Newcastle upon Tyne, U.K., 2010, pp. 341–346.

[21] *Wireless LAN Medium Access Control (MAC) and Physical Layer (PHY) Specifications: Higher-Speed Physical Layer Extension in the 2.4 GHz Band*, IEEE Std. 802.11b, 1999.

[22] T. Guo and R. Carrasco, "CRBAR: Cooperative relay-based auto rate MAC for multirate wireless networks," *IEEE Trans. Wireless Commun.*, vol. 8, no. 12, pp. 5938–5947, Dec. 2009.

[23] V. Tarokh, N. Seshadri, and A. R. Calderbank, "Space–time codes for high data rate wireless communication: Performance criterion and code construction," *IEEE Trans. Inf. Theory*, vol. 44, no. 2, pp. 744–765, Mar. 1998.

[24] E. Zehavi, "8-PSK trellis codes for a Rayleigh channel," *IEEE Trans. Commun.*, vol. 40, no. 5, pp. 873–884, May 1992.

[25] G. Caire and E. Biglieri, "Bit-interleaved coded modulation," *IEEE Trans. Inf. Theory*, vol. 44, no. 3, pp. 927–946, May 1998.

[26] L. R. Bahl, J. Cocke, F. Jelinek, and J. Raviv, "Optimal decoding of linear codes for minimizing symbol error rate," *IEEE Trans. Inf. Theory*, vol. IT-20, no. 2, pp. 284–287, Mar. 1974.

[27] S. ten Brink, J. Speidel, and R. H. Yan, "Iterative demapping for QPSK modulation," *Electron. Lett.*, vol. 34, no. 15, pp. 1459–1460, Jul. 1998.

[28] G. J. Foschini and M. J. Gans, "On limits of wireless communications in a fading environment when using multiple antennas," *Wirel. Pers. Commun.*, vol. 6, no. 3, pp. 311–335, Mar. 1998.

Li Chen (M'08), photograph and biography not available at the time of publication.

Rolando Carrasco, photograph and biography not available at the time of publication.

Ian Wassell, photograph and biography not available at the time of publication.